
STRUCTURAL ANALYSIS OF LIPIDS BY NUCLEAR MAGNETIC RESONANCE

A PREPRINT

Heather R. MacGregor

Department of Chemistry and Biochemistry
University of California, Santa Barbara
Santa Barbara, CA 93117
macgregor@ucsb.edu

January 19, 2020

ABSTRACT

The objective of this experiment is to use Nuclear Magnetic Resonance (NMR) spectroscopy to identify the components of and determine the qualitative composition of a mixture made from two fairly similar fatty acid methyl esters. This experiment introduces multi-dimensional NMR techniques, as well as methods for their analysis. NMR is an attractive method for qualitative analysis of complex mixtures of lipids, which has important applications in the food sciences.

1 Experimental Design

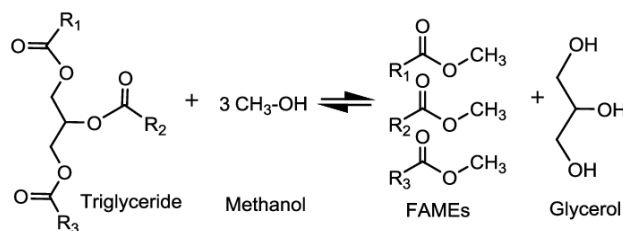


Figure 1: Reaction between triglyceride and methanol to generate fatty acid methyl esters (FAMES) and glycerol.

Recently, high-resolution NMR spectroscopy has gained popularity as a method to investigate the composition of mixtures present in oils and fats. It is particularly advantageous with respect to other spectroscopic methods due to the large amount of information that can be extracted from a single NMR spectrum. Additionally, it does not require chemical treatments. The aliphatic side chains of each fatty acid may be identified by their unique NMR signals in both ¹H and ¹³C-¹H NMR spectra. ¹³C-¹H NMR spectra allows for both the direct identification of fatty acids esterified to the glycerol backbone, as well as the amounts of each fatty acid esterified to the α and β positions on the glycerol backbone.

Fatty acid methyl esters (FAMES) are composed of the fatty acid aliphatic chain esterified to a methyl group. The ¹H NMR spectrum of a FAME is virtually indistinguishable to that of its corresponding FA except for the strong singlet peak caused by the methyl ester protons around 3.7 ppm. One advantage of ¹H NMR is the high natural abundance and magnetic moment of ¹H nuclei, allowing for the quick acquisition of ¹H NMR spectra with a good signal-to-noise ratio. Thus, ¹H NMR spectra has been widely considered the tool of choice for the determination of fatty acid composition by NMR spectroscopy. The main disadvantage of ¹H NMR is that the homonuclear spin coupling of protons leads to a low dispersion; thus, no distinct NMR chemical shifts will appear according to the position of the acyl fatty group on the glycerol backbone. This would be required for the determination of the positional distribution of different classes of fatty acids on the glycerol backbone, but will not provide an issue in the qualitative analysis of fatty acid methyl

esters. However, despite the sensitivity of ^1H NMR spectra, they do not provide enough spectral resolution to resolve signals from components of a complicated mixture. Overall, ^1H NMR alone will not provide sufficient information to determine the structure of the two similar FAME components of the mixture.

The ^{13}C NMR chemical shifts of lipids can be grouped in four regions: the carbonyl and carboxyl carbons in the region of 172–178 ppm, unsaturated carbons of 124–134 ppm, the glycerol backbone carbons of 60–72 ppm and aliphatic carbons of 10–35 ppm.

The signal-to-noise ratio in NMR spectroscopy is dependent on concentration in addition to other factors:

$$\frac{S}{N} \approx \frac{N \gamma_n^{\frac{5}{2}} B_0^{\frac{3}{2}} T_2 \sqrt{ns}}{T} \quad (1)$$

where N is concentration, γ_n is the magnetogyric ratio of the nucleus, B_0 is the strength of the external field, T_2 is the transverse relaxation time, ns is the number of transients, and T is temperature. From this, one would expect that the detection limit for ^{13}C will be much higher than for ^1H . Although this limitation can be overcome simply by taking more scans for ^{13}C , this significantly increases the time required for data acquisition. Additionally, the acquisition of each individual spectrum must be performed with a long time delay between averages in order to allow for total spin relaxation of the ^{13}C nuclei. Overall, this results in the collection of ^{13}C NMR spectra being highly time-consuming.

In a mixture of FAMES, all fatty acyl chains are esterified to a common moiety, in this case the methyl group. The signal's intensity (and area under the curve) is directly proportional to the specific number of protons in the sample producing the signal at that specific chemical shift. Thus, the fatty acid composition may be determined through the ratio of the areas of the characteristic signals of each fatty acyl chain.

Heteronuclear single-quantum correlation spectroscopy (HSQC) detects correlations between nuclei of two different types which are separated by one bond, while heteronuclear multiple bond correlation spectroscopy (HMBC) detects those separated by two and three bonds, while suppressing the results seen in HSQC. Interpretation of the resulting spectra from these two correlation NMR techniques will allow for a great deal of information regarding the structural features of each FAME to be determined. Identification of the two FAMES in the mixture will then allow for the ratio to be calculated.

Signal	Chemical Shift (ppm)
ω -1	14.1
ω -2	22.8
ω -3	32.1
C ₁	174.1
C ₂	34.2
C ₃	25.1
glycerol ¹	68.9 & 62.1
olefinic	127–132
allylic	27.3 & 25.6

Table 1: Easily recognized chemical shifts of lipids in ^{13}C NMR spectra.

Overall, ^1H NMR is the most appropriate method for quantitative determination of the composition of a mixture of two FAMES due to its quick data acquisition and straightforward analysis. However, time permitting, ^{13}C NMR spectra may also be taken as this will provide further structural information.

2 Materials and Methods

2.1 Sample preparation

NMR samples were prepared by dissolving 80 μL of a mixture of two unknown fatty acid methyl esters in 720 μL of deuterated chloroform in a 5 mm NMR tube (Wilmad).

¹Not applicable for a mixture of FAMES.

2.2 1D NMR experiments

^1H NMR spectra was obtained at 400 MHz on an Agilent (Santa Barbara, CA) 400MR DD2 NMR spectrometer with CDCl_3 as solvent. 32052 transients were accumulated and averaged over 8 scans. An acquisition time of 2.5 s, relaxation delay of 4.8 s, and sweep width of 6.4102 kHz were employed in the spectral measurements.

^{13}C NMR spectra was obtained at 500 MHz on a Varian (Santa Barbara, CA) Unity Inova 500 NMR spectrometer with CDCl_3 as solvent. 78590 transients were accumulated and averaged over 200 scans. An acquisition time of 1.0 s, relaxation delay of 1.0 s, and sweep width of 30.1659 kHz were employed in the spectral measurements.

2.3 2D NMR experiments

^1H - ^{13}C gHSQC NMR spectra was obtained at 600 MHz on a Varian (Santa Barbara, CA) Unity Inova 600 NMR spectrometer with CDCl_3 as solvent. 1024 and 320 transients were accumulated for ^1H and ^{13}C , respectively, and averaged over 4 scans. An acquisition time of 0.142 s, relaxation delay of 1.6 s, and sweep width of 3.5977 and 24.1253 kHz were employed for ^1H and ^{13}C , respectively, in the spectral measurements.

^1H gTOCSY NMR spectra was obtained at 600 MHz on a Varian (Santa Barbara, CA) Unity Inova 600 NMR spectrometer with CDCl_3 as solvent. 2048 transients were accumulated and averaged over 4 scans. An acquisition time of 0.184 s, relaxation delay of 1.6 s, and sweep width of 3.6088 kHz were employed in the spectral measurements.

^1H gCOSY NMR spectra was obtained at 600 MHz on a Varian (Santa Barbara, CA) Unity Inova 600 NMR spectrometer with CDCl_3 as solvent. 1024 transients were accumulated and averaged over 4 scans. An acquisition time of 0.141 s, relaxation delay of 1.6 s, and sweep width of 3.6088 kHz were employed in the spectral measurements.

2.4 Data analysis

Raw data was processed and analyzed using Mnova 14.1.0.¹ Initial peak assignments for all collected spectra were performed manually with consideration to literature data. Peaks (excluding solvent) from the one-dimensional ^1H and ^{13}C NMR spectra were used to query the Spectral Database for Organic Compounds (SDBS).² For each hit compound, both simulated and experimental spectra were compiled and compared to those of the mixture.^{1,2,3,4} The percent composition of the mixture was determined by the normalized integration values of the protons of the ester methoxy group (3.6-3.7 ppm) were correlated with those of the various protons of the alkyl chain.

3 Results and Discussion

3.1 ^1H NMR

^1H NMR (400 MHz, CDCl_3) δ 5.40 – 5.25 (m, 2H), 3.64 (s, 2H), 2.28 (t, J = 7.5 Hz, 1H), 2.00 (dq, J = 9.7, 6.7 Hz, 3H), 1.66 – 1.56 (m, 1H), 1.28 (s, 6H), 1.38 – 1.22 (m, 5H), 0.91 – 0.82 (m, 2H).

Assignment	Shift	Range	Hs	Integral	J	Class	Normalized	Absolute
H	0.86	0.91 .. 0.82	2(16)	2.04		m	1.20	8479.37
G	1.28	1.31 .. 1.26	6(48)	5.96		s		
F	1.27	1.38 .. 1.22	5(40)	5.03		m	6.33	44797.88
E	1.60	1.66 .. 1.56	1(8)	1.01		m	0.83	5877.03
D	2.00	2.08 .. 1.94	3(24)	2.80	6.75, 6.75, 6.54, 9.72	dq	1.61	11423.43
C	2.28	2.32 .. 2.24	1(8)	1.40	7.55, 7.55	t	0.83	5872.72
		2.91 .. 2.64					0.22	1589.17
B	3.64	3.66 .. 3.62	2(16)	2.04		s	1.20	8488.48
A	5.33	5.40 .. 5.25	2(16)	1.71		m	1.00	7059.00

Table 2: ^1H NMR of the binary mixture of unknown fatty acid methyl esters.

From the proton NMR alone, we are able to identify the ratio of one of the individual components to the mixture by comparison of the signal produced by 2H at about 2.6 ppm and that of the 6H in the methyl ester groups of the 2

FAMEs:

$$\frac{N^{(1)}}{n_H^{(1)}} \times \frac{n_H^{(2)}}{N^{(2)}} = \frac{0.22}{2} \times \frac{6}{1.20}$$

$$= 55\% \quad \longrightarrow \text{FAME}^{(1)}$$

$$\approx 45\% \quad \longrightarrow \text{FAME}^{(2)}$$

3.2 ^{13}C NMR

^{13}C NMR (126 MHz, CDCl_3) δ 174.34, 130.27, 130.11, 130.07, 129.83, 128.14, 128.01, 77.41, 77.16, 76.91, 51.48, 34.18, 32.69, 31.89, 31.63, 29.84, 29.78, 29.69, 29.45, 29.26, 29.23, 29.18, 29.09, 27.32, 27.30, 27.28, 27.25, 25.73, 25.05, 22.76, 22.68, 22.62, 14.18, 14.15.

	ppm	Intensity	Width	Area	Range	Normalized	Absolute
1	174.34	33.3	2.72	593.32	174.47 .. 174.20	0.98	611.41
2	130.27	35.6	2.72	658.92	130.41 .. 130.16	1.15	717.00
3	130.11	38.7	2.72	652.83	130.16 .. 129.94	3.96	2477.27
4	130.07	107.9	2.72	1982.38			
5	129.83	103.8	2.72	1899.38	129.94 .. 129.71	3.02	1891.00
6	128.14	39.2	2.72	721.40	128.29 .. 127.89	2.08	1299.14
7	128.01	33.7	2.72	621.15	51.62 .. 51.36	2.61	1630.72
8	51.48	87.6	3.18	1886.20			
9	34.18	161.4	2.81	2892.17	34.30 .. 34.06	4.38	2738.23
10	32.69	2.2	5.05	81.31	32.01 .. 31.77	2.60	1628.12
11	31.89	97.5	2.72	1695.57	31.77 .. 31.51	1.03	647.56
12	31.63	34.0	2.70	578.87			
13	29.84	108.4	2.72	1896.58	29.98 .. 29.60	7.79	4876.33
14	29.78	122.1	2.72	2193.81			
15	29.69	46.2	2.72	841.17	29.60 .. 29.37	1.38	861.48
16	29.45	36.7	2.68	641.63	29.37 .. 28.92	17.56	10990.23
17	29.26	171.2	2.72	3098.61			
18	29.23	166.9	2.84	3097.81			
19	29.18	145.8	3.15	3033.29			
20	29.09	109.5	2.72	1976.96			
21	27.32	108.8	2.51	1787.80	27.46 .. 27.04	8.82	5518.78
22	27.30	45.6	2.87	821.47			
23	27.28	40.9	2.26	523.82			
24	27.25	124.3	2.72	2277.39			
25	25.73	43.0	2.72	777.07	25.87 .. 25.60	1.18	735.29
26	25.05	160.2	2.72	2859.57	25.38 .. 24.59	4.89	3057.15
27	22.76	88.1	2.72	1572.00	22.88 .. 22.44	3.34	2092.56
28	22.68	33.1	2.72	614.90			
29	22.62	3.1	6.20	145.73			
30	14.18	77.8	2.90	1515.26			
31	14.15	28.1	2.71	500.98	14.32 .. 13.91	3.09	1933.38

Table 3: ^{13}C NMR of the binary mixture of unknown fatty acid methyl esters.

3.3 Heteronuclear 2D NMR

3.3.1 gHSQC

The bis-allylic protons, $=\text{HC}-\text{CH}_2-\text{CH}=\text{}$, in polyenoic fatty acids and esters are in a characteristic region of 2.60–2.85 ppm due to the effect of the magnetic anisotropy of the double bonds. They are more deshielded due to a larger number of double bonds.

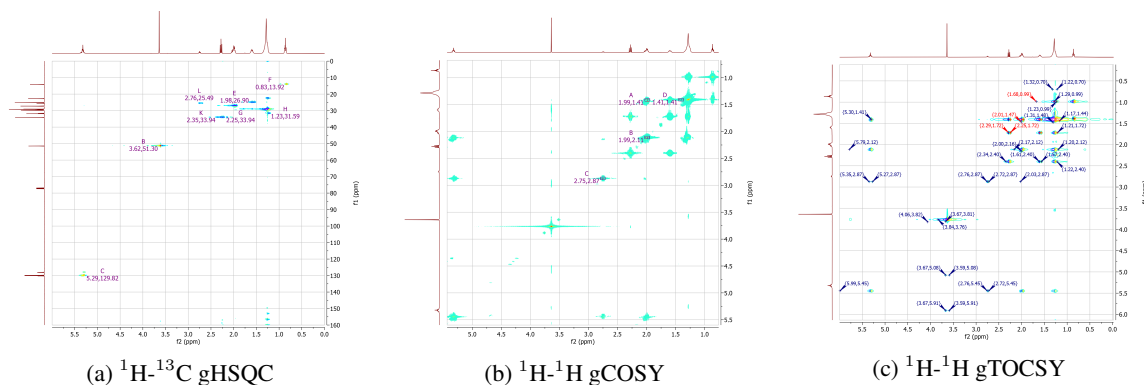


Figure 2: Results of multi-dimensional spectral measurements of the binary mixture of FAMES.

Name	f_1 Shift	f_2 Shift	Group _{MO}	Group _{ML}
O	127.94	5.28	-CH=CH-	-CH=CH-CH ₂ -CCH=CH-
N	25.49	2.69	—	-CH=CH-CH ₂ -CH=CCH-
L	25.49	2.76	—	-CH=CH-CH ₂ -CH=CCH-
K	33.94	2.35	-CH ₂ -	—
J	24.87	1.57	-CH ₂ -	-CH ₂ -
I	22.36	1.24	-CH ₂ -	-CH ₂ -
H	31.59	1.23	-CH ₂ -CH ₂ -CH ₂ -	-CH ₂ -CH ₂ -CH ₂ -
G	33.94	2.25	—	-CH ₂ -
F	13.92	0.83	-C-C-H ₃	-C-C-H ₃
E	26.9	1.98	-CH ₂ -CH ₂ -CH=CH-CH ₂ -CH ₂ -	-CH ₂ -CH ₂ -CH=CH-CH ₂ -CH ₂ -CH ₂ -
D	29.56	1.28	-CH ₂ -CH ₂ -CH ₂ -CH ₂ -	-CH ₂ -CH ₂ -CH ₂ -CH ₂ -
C	129.82	5.29	—	-CH=CH-CH ₂ -CH=CH-
B	51.3	3.62	-COO-CH ₃	-COO-CH ₃
A	28.93	1.25	-CH ₂ -CH ₂ -CH ₂ -CH ₂ -CH ₂ -CH ₂ -CH ₂ -CH ₂ -	-CH ₂ -CH ₂ -CH ₂ -CH ₂ -CH ₂ -

Table 4: ^1H - ^{13}C gHSQC ($f_1 = ^{13}\text{C}$; $f_2 = ^1\text{H}$); peaks auto-detected by MNova.¹

3.4 Homonuclear 2D NMR

3.4.1 ^1H - ^1H gTOCSY

^1H - ^1H NMR ((600, 600) MHz, CDCl_3) δ (5.99 5.45), (5.79 2.12), (5.76 5.08), (5.35 2.87), (5.30 1.41), (5.27 2.87), (4.06 3.82), (3.84 3.76), (3.69 3.89), (3.69 3.72), (3.67 3.06), (3.67 3.81), (3.67 5.08), (3.67 5.78), (3.67 5.91), (3.63 0.12), (3.59 3.06), (3.59 5.08), (3.59 5.78), (3.59 5.91), (3.57 3.72), (2.76 2.15), (2.76 2.87), (2.76 5.45), (2.72 2.15), (2.72 2.87), (2.72 5.45), (2.63 3.64), (2.34 2.40), (2.31 0.42), (2.31 1.11), (2.29 1.41), (2.29 1.72), (2.26 2.46), (2.25 1.41), (2.25 1.72), (2.23 0.42), (2.17 2.12), (2.13 2.87), (2.02 0.70), (2.02 2.25), (2.01 1.47), (2.01 5.49), (2.00 2.16), (2.00 1.41), (1.96 1.41), (1.94 0.70), (1.73 1.02), (1.73 1.82), (1.68 0.99), (1.63 1.10), (1.61 2.40), (1.60 1.41), (1.60 1.72), (1.57 1.41), (1.57 1.72), (1.57 2.40), (1.56 1.23), (1.32 0.70), (1.32 1.10), (1.31 1.48), (1.31 1.82), (1.31 2.16), (1.29 0.99), (1.28 1.49), (1.23 0.99), (1.23 1.10), (1.23 1.82), (1.22 0.70), (1.22 1.67), (1.22 2.40), (1.21 1.48), (1.21 1.72), (1.20 2.12), (1.17 1.44), (0.96 1.62), (0.90 0.93), (0.89 1.04), (0.89 2.66), (0.87 1.39), (0.83 1.04), (0.83 1.39), (0.81 1.83), (0.81 2.67), (0.51 2.14), (0.25 2.42), (-19.94 5.45).

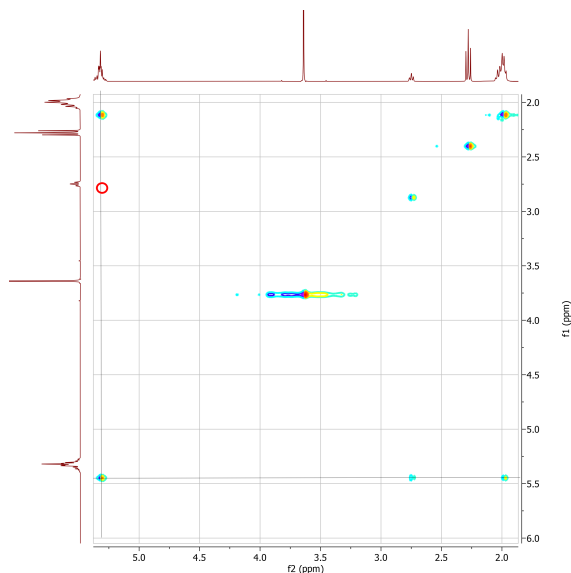
gTOCSY, or (Gradient-enhanced) TOverlaid Correlation Spectroscopy, is a two-dimensional homonuclear NMR technique that provides correlations between protons that are "connected" through an uninterrupted pattern of coupling constants. Importantly, it is not based on long-range coupling constants.

Cross-peaks δ_1 (5.38, 2.07) and δ_2 (5.38, 2.79) are methylene proton couplings in the acyl chain to the unsaturated site protons. Cross-peak δ_1 arises from spin-spin coupling between olefinic (-CH=CH-) and allylic methylene protons (-CH₂-CH₂=CH-) and thus appears only if the methylene protons is adjacent to only one unsaturated site proton. Crosspeak δ_2 arises from spin-spin coupling between olefinic (-CH=CH-) and diallylic methylene protons (-CH=CH₂-CH-) and appears if there are at least two unsaturated sites and the methylene protons are located between the unsaturated site protons. The ratio of cross-peaks δ_2/δ_1 is thus a measure of the degree of unsaturation, as seen in Table 5.²

Fatty acid	δ_2/δ_1 ratio
Oleic (18:1)	0.0
Linoleic (18:2)	1.3
Linolenic (18:3)	2.7
Arachidonic (20:4)	4.0

Table 5: δ_2/δ_1 Cross-Peak Volume Ratios for Fatty Acid Standards.²

Visual analysis of the experimental ^1H - ^1H gTOCSY spectrum reveals a very weak δ_2 (f_2, f_1) in comparison to δ_2 (f_1, f_2). However, the volume of δ_1 (f_2, f_1) approximately that of δ_1 (f_1, f_2). This indicates there is less δ_2 coupling than δ_1 coupling present in the mixture, which further supports the proposal that the binary mixture contains methyl oleate and methyl linoleate.

Figure 3: δ_2/δ_1 Cross-Peak analysis of experimental ^1H - ^1H gTOCSY spectrum.

3.5 ^1H - ^1H gCOSY

In a COSY experiment, cross-peaks correspond to protons that have 3-bond proton-proton scalar coupling, $^3J_{HH}$. Standard COSY experiments require phase cycling to remove unwanted signals and thus can be quite time consuming. This can be largely circumvented using gradient-selected COSY (gCOSY), which utilizes pulsed field gradients to destroy unwanted magnetization and hence their associated signals (axial peaks).

Assign.	f_1 Shift	f_2 Shift	Group
D	1.41	1.41	$-\text{CH}_2-\text{CH}_2-\text{CH}_2-$
C	2.87	2.75	$-\text{CH}_2-\text{CH}=\text{CH}-\text{CH}_2-\text{CH}=\text{CH}-$
B	2.11	1.99	$-\text{CH}_2-\text{CH}_2-\text{CH}_2-\text{CH}=\text{CH}-$
A	1.41	1.99	$-\text{CH}=\text{CH}-\text{CH}_2-\text{CH}_2-\text{CH}_2-$

Table 6: ^1H - ^1H gCOSY ($f_1 = ^1\text{H}$; $f_2 = ^1\text{H}$); peaks auto-detected by MNOVA.¹

3.6 Reference Spectra

Based on the experimental results, the components of the binary mixture were identified as methyl oleate and methyl linoleate. To further support this argument, experimental reference spectra and theoretical spectra were simulated

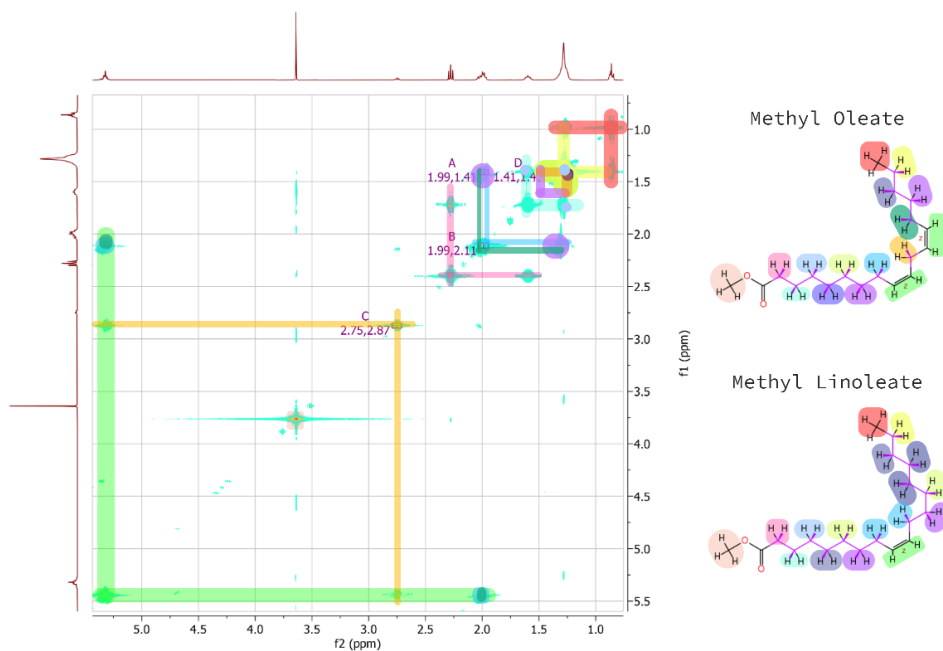


Figure 4: Annotated ^1H - ^1H gCOSY spectrum. Groups of protons are color coded accordingly.

for both individual components. Both qualitative and quantitative comparison between the spectra of the individual components and that of the mixture confirm the identification.

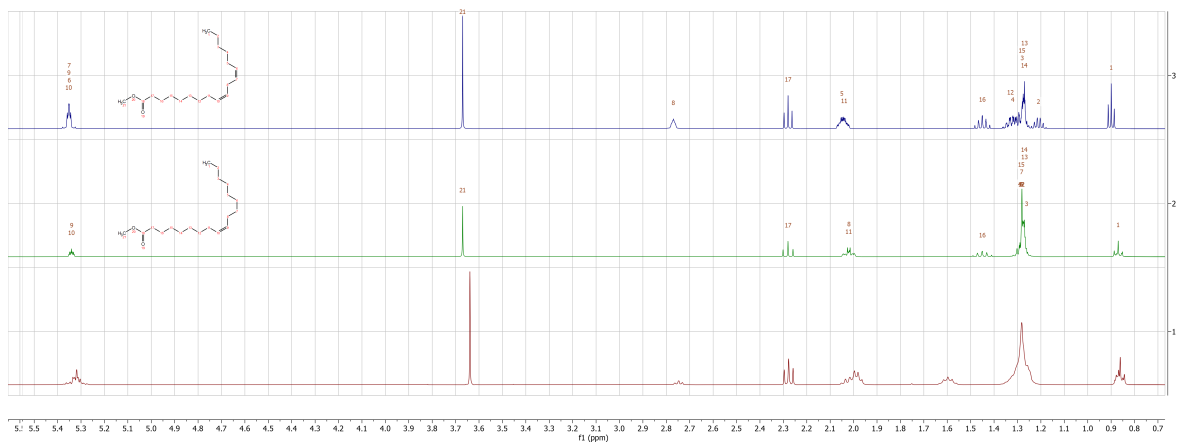


Figure 5: Theoretical ^1H NMR spectra of methyl linoleate (top; blue) and methyl oleate (middle; green). Experimental spectra of the binary mixture of fatty acid methyl esters (bottom; red).

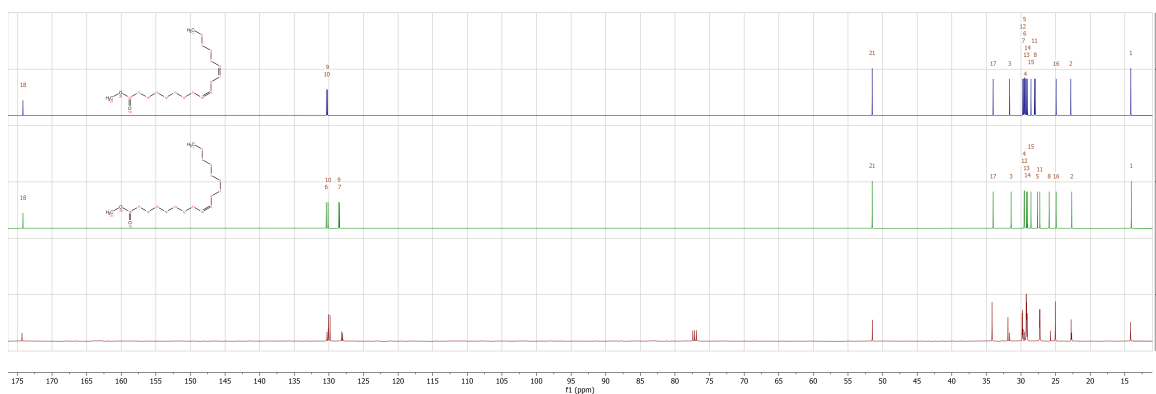
4 Discussion

The ^1H NMR spectra of many fatty acids shows characteristic signals that can be used to quantify the amount of saturated, mono-, double-, and triple-unsaturated chains in the sample. For example (Fig. 7), the ^1H NMR spectrum for palmitic acid shows the terminal methyl group ω_1 , $-\alpha\text{CH}_2$, $-\beta\text{CH}_2$, and the remaining methylene CH_2 groups overlapping at approximately 1.3 ppm, whereas oleic acid has two olefinic hydrogens (coupled to the double-bonded C_9 and C_{10}) that produces a signal around 5.3 ppm. Additionally, the presence of the double bond results in the peak corresponding to the allylic CH_2 to be shifted upfield. The four olefinic hydrogens present in linoleic acid generate a

Assign.	Shift	Range	H's	Integral	J's	Class
K	0.90	0.93 .. 0.87	2	1.54	6.40, 6.40	t
J	1.23	1.28 .. 1.16	2	1.99		m
I	1.28	1.31 .. 1.25	3	3.08		m
H	1.31	1.34 .. 1.28	2	1.97		m
G	1.34	1.38 .. 1.31	1	1.00		m
F	1.45	1.50 .. 1.40	1	1.03		m
E	2.05	2.09 .. 2.00	2	2.05	1.23, 3.16, 5.40, 8.18, 10.92	dddd
D	2.28	2.31 .. 2.25	1	1.01	8.47, 8.47	t
C	2.77	2.81 .. 2.73	1	1.00	0.92, 0.92, 2.16, 3.87, 4.93	dddt
B	3.67	3.69 .. 3.65	1	1.19		s
A	5.35	5.40 .. 5.31	2	2.14	1.35, 2.83, 4.08	ddd

Table 7: Simulated ^1H NMR of methyl linoleate.

Assign.	Shift	Range	H's	Integral	J's	Class
G	0.87	0.92 .. 0.83	2	1.53		m
F	1.27	1.34 .. 1.22	10	10.16		m
E	1.45	1.50 .. 1.40	1	1.04		m
D	2.02	2.06 .. 1.98	2	2.09		m
C	2.28	2.31 .. 2.24	1	1.04	8.49, 8.49	t
B	3.67	3.69 .. 3.65	1	1.14		s
A	5.34	5.37 .. 5.31	1	1.01	1.41, 3.13, 4.45	ddd

Table 8: Simulated ^1H NMR of methyl oleate.Figure 6: Theoretical ^{13}C NMR spectra of methyl linoleate (top; blue) and methyl oleate (middle; green). Experimental spectra of the binary mixture of fatty acid methyl esters (bottom; red). The peak at 77ppm corresponds to the solvent (CDCl_3).

peak structure at the same position, but with a greater degree of splitting. Additionally, the bis-allylic group at C_8 yields a triplet around 2.7 ppm. These unique signals allow for the quantification the fatty acid profile of complex mixtures of oils.

4.1 qNMR in QC of Food and Drugs

Traditionally, NMR has been an analytical technique applied in the verification and elucidation of molecular structures and for the determination of sample purity or yield. However, the demands of emerging fields have accelerated the evolution of the technique. A pertinent example is the application of NMR to the quantitative determination of the fatty acid profile in complex mixtures of oils, information which is used to classify the quality of edible oils and must be printed on the label of edible oils in the European Union (Regulation 1169/2011) since 2014.⁵ Recently, the ^1H -NMR spectra of extra virgin olive oils (EVOO) in order to differentiate EVOO based on the presence of specific aldehydes, which would allow for better quality control of adulterated samples.^{6,7,8,9} Application of principle component analysis (PCA) to spectral data can accurately predict the geographical origin and variety of olive from which the oil was produced.^{8,10,11}

In addition to the food sciences, ^1H NMR has enjoyed rising applicability in metabolomics. Untargeted metabolomics studies consist of collection of 1D ^1H NMR spectra of cell lysates and/or biofluid samples that serve as a fingerprint of the state of the metabolome (Fig. 9). PCA and other statistical methods are then used to pinpoint differences between multiple classes of samples (i.e. drug treated vs untreated). Then, the metabolites that correspond to the primary sources of the observed spectral differentiations may be identified. Additionally, the *in vivo* mechanism of action of a potential

Methyl Linoleate						Methyl Oleate					
Assign.	Shift	Range	Hs	J	Class	Assign.	Shift	Range	Hs	J	Class
H	0.86		3	7.0	t	H	0.86		3	7.0	t
F	1.25	1.21-1.32	10	7.7, 7.0	tt	G	1.25	1.19-1.32	16	7.7, 7.0	tt
	1.28			7.0	h		1.28			7.0	h
	1.25			7.0	quint		1.24			7.0	quint
	1.25	1.38-1.47	4	7.0, 6.6	tt		1.23	1.38-1.47	4	7.0	quint
	1.26			7.0, 6.6	tt		1.23			7.0	quint
	1.42			7.4, 7.0	tt		1.24			7.0	quint
	1.43			7.4, 7.0	tt		1.25			7.0	quint
E	1.55	1.92-2.01	2	7.7, 7.4	tt	E	1.26	1.91-2.01	2	7.0	quint
D	1.96			7.4, 7.4	td		1.43			7.7, 7.4	tt
	1.96			7.4, 7.4	td		1.43			7.7, 7.4	tt
C	2.25		2	7.4	t	D	1.55		2	7.7, 7.4	tt
	2.63			7.4	t		1.97			7.4	q
B	3.63		3		s		1.95			7.4	q
A	5.35	5.30-5.41	4	11.0, 7.4	dt	C	2.25		2H	7.4	t
	5.36			11.0, 7.4	dt	B	3.63		3		s
	5.35			11.0, 7.4	dt	A	5.33	5.28-5.38	2	11.0, 7.4	dt
	5.35			11.0, 7.4	dt		5.33			11.0, 7.4	dt

Table 9: Simulated ^1H NMR of methyl linoleate (δ 0.86 (3H, t, $J = 7.0$ Hz), 1.21-1.32 (10H, 1.25 (tt, $J = 7.7, 7.0$ Hz), 1.28 (h, $J = 7.0$ Hz), 1.25 (quint, $J = 7.0$ Hz), 1.25 (tt, $J = 7.0, 6.6$ Hz), 1.26 (tt, $J = 7.0, 6.6$ Hz)), 1.38-1.47 (4H, 1.42 (tt, $J = 7.4, 7.0$ Hz), 1.43 (tt, $J = 7.4, 7.0$ Hz)), 1.55 (2H, tt, $J = 7.7, 7.4$ Hz), 1.92-2.01 (4H, 1.96 (td, $J = 7.4, 7.4$ Hz)), 2.25 (2H, t, $J = 7.4$ Hz), 2.63 (2H, t, $J = 7.4$ Hz), 3.63 (3H, s), 5.30-5.41 (4H, 5.35 (dt, $J = 11.0, 7.4$ Hz), 5.36 (dt, $J = 11.0, 7.4$ Hz), 5.35 (dt, $J = 11.0, 7.4$ Hz), 5.35 (dt, $J = 11.0, 7.4$ Hz))) and methyl oleate (δ 0.86 (3H, t, $J = 7.0$ Hz), 1.19-1.32 (16H, 1.25 (tt, $J = 7.7, 7.0$ Hz), 1.28 (h, $J = 7.0$ Hz), 1.24 (quint, $J = 7.0$ Hz), 1.23 (quint, $J = 7.0$ Hz), 1.24 (quint, $J = 7.0$ Hz), 1.25 (quint, $J = 7.0$ Hz), 1.26 (quint, $J = 7.0$ Hz)), 1.38-1.47 (4H, 1.43 (tt, $J = 7.4, 7.0$ Hz), 1.43 (tt, $J = 7.4, 7.0$ Hz)), 1.55 (2H, tt, $J = 7.7, 7.4$ Hz), 1.91-2.01 (4H, 1.97 (q, $J = 7.4$ Hz), 1.95 (q, $J = 7.4$ Hz)), 2.25 (2H, t, $J = 7.4$ Hz), 3.63 (3H, s), 5.28-5.38 (2H, 5.33 (dt, $J = 11.0, 7.4$ Hz), 5.33 (dt, $J = 11.0, 7.4$ Hz))).

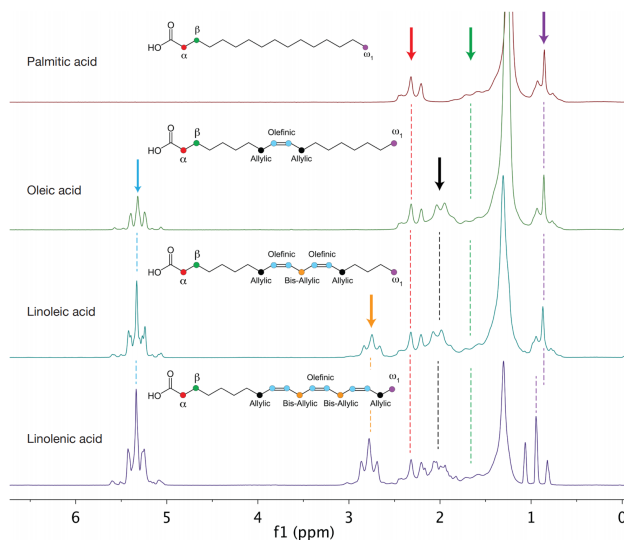


Figure 7: ^1H NMR spectra of palmitic, oleic, linoleic, and linolenic acid measured with a Spinsolve 60 MHz in a single scan. The samples were dissolved in CDCl_3 at a concentration of 0.5M for palmitic acid (close to the solubility limit) and 1M for the rest.

lead may be deduced by comparing the observed changes in the metabolome to those observed when treated with a drug with a known target.¹²

The experiment provided hands-on experience with a simple, effective technique that has recently enjoyed wide applicability outside of analytical research.

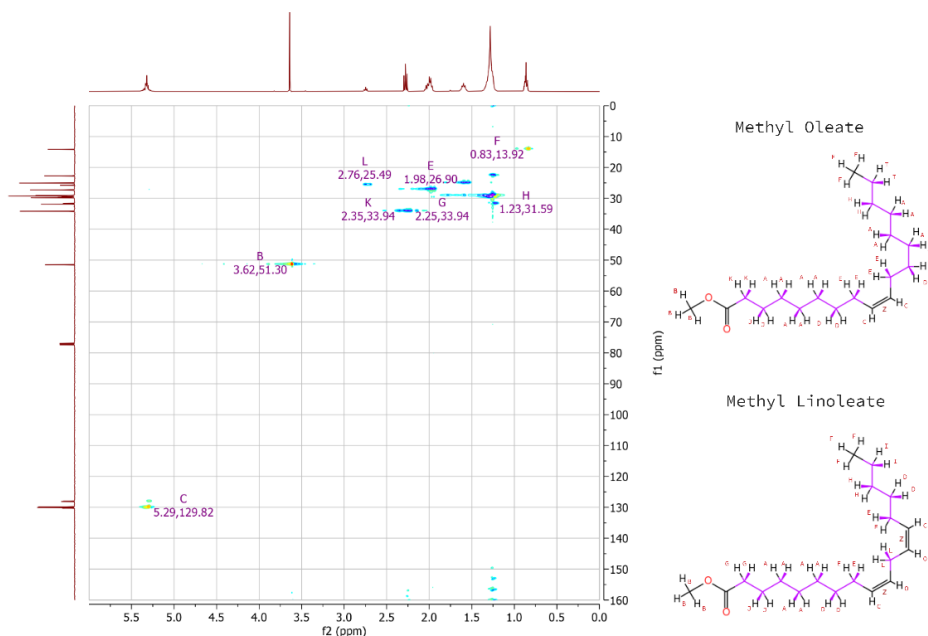


Figure 8: Caption

Methyl Oleate				Methyl Linoleate		
C	Assignment	Shift	Area	Assignment	Shift	Area
1	H	51.77671	1886.20	H	51.77671	1886.20
2	A	173.53737	593.32	A	173.53737	593.32
3	I	33.84391	2892.17	I	33.84391	2892.17
4	Z	25.28	2859.57	Z	25.28	2859.57
5	N	29.21543	2193.81	N	29.21543	2193.81
6	P	28.96564	641.63	P	28.96564	641.63
7	Q	28.965	3098.61	Q	28.965	3098.61
8	R	28.95755	3097.81	R	28.95755	3097.81
9	V (?)	28.71406	821.47	V (?)	28.71406	821.47
10	D or E	129.9	1982.38 or 1899.38	B or C	130.525	658.92 or 652.83
11	F or G	128.56666	721.40 or 621.15	B or C	130.525	658.92 or 652.83
12	Y	25.84	777.07	X (?)	28.71406	2277.39
13	F or G	128.56666	721.40 or 621.15	R	28.95755	3097.81
14	D or E	129.9	1982.38 or 1899.38	Q	28.965	3098.61
15	W (?)	28.71406	523.82	P	28.96564	641.63
16	O	29.02818	841.17	M	29.35859	1896.58
17	K or L	31.63461	1695.57 or 578.87	J	32.40308	81.31
18	AA or BB	22.61947	1572.00 or 614.90	AA or BB	22.61947	1572.00 or 614.90
19	CC	14.00088	1515.26	CC	14.00088	1515.26

Table 10: Simulation of ^{13}C NMR of methyl oleate (δ (ppm) 51.77671, 22.61947, 173.53737, 14.00088, 28.71406, 28.965, 25.28, 28.96564, 28.71406, 29.35859, 28.95755, 130.525, 32.40308, 29.21543, 33.84391, 28.965, 28.96564, 28.95755, 130.525) and methyl linoleate (δ (ppm) 51.77671, 22.61947, 173.53737, 14.00088, 28.71406, 28.965, 25.28, 28.96564, 28.71406, 29.35859, 28.95755, 130.525, 32.40308, 29.21543, 33.84391, 28.965, 28.96564, 28.95755, 130.525).

4.2 Potential Improvements

With the exception of the ^1H NMR spectrum, the spectra collected here were not explicitly required to determine the structure and composition of the FAMES present in the binary mixture. However, the collection and analysis of multi-dimensional spectra allows for one to both gain experience in such analyses and attain a greater degree of confidence in the proposed structures of each component.

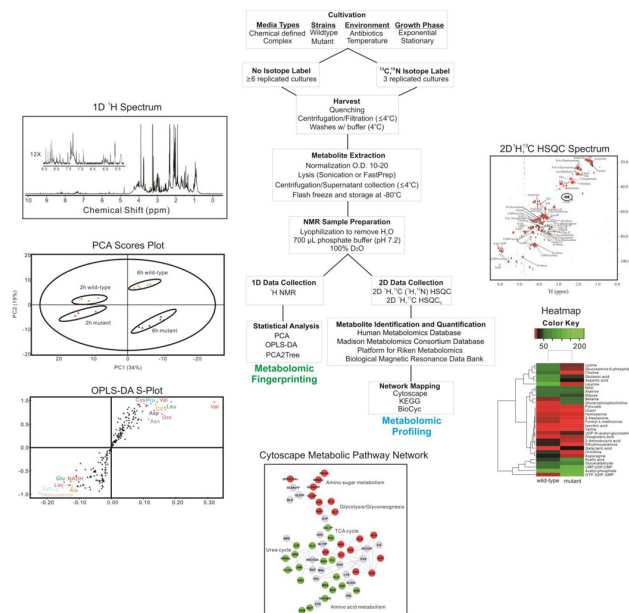


Figure 9: A flowchart of a typical protocol used in the NMR analysis of bacterial metabolomes.¹²

First, the spectrum must have an adequate signal to noise ratio to support the level of accuracy required for the specific experiment. In the analysis shown here, this factor does not present a significant issue, but may be improved by increasing the number of scans.

Quantitative NMR relies on the principle that the integrals of resonance peaks are proportional to the number of nuclei that comprise the resonances. Additionally, the absolute area of the integrals is dependent on spectrometer and sample properties (relaxation time, pulse excitation, broad-band decoupling). The effect of relaxation time can be ignored with a sufficiently long acquisition time or may be measured and factored in directly.¹³ One can account for the effect of other factors by comparison to a calibration standard. Here, we use the popular internal standard TMS; because the quantification is dependent on the ratio between the target and reference peak integrals, any errors associated with the generation or measurement of the reference peak (including sample preparation, spectra processing, and spectra analysis) have the same relative impact on all quantified components.⁷ Additionally, because peaks that are closely spaced cannot be accurately integrated by the usual method, and are thus avoided for determination of the quantitative composition of the mixture.

In the ^{13}C spectra, each signal has corresponding " ^{13}C satellites" located $\pm J_{\text{C-H}}/2$ (about 115-135 Hz) from the center of the peak. This results in a loss of about 1.1% of the area under the peak. In future experiments, it may be avoided by ^{13}C -decoupling, which compresses the satellites into the central peak.

5 Conclusion

This experiment successfully identified the composition of the unknown binary mixture to be 45:55 methyl oleate:methyl linoleate using NMR techniques. As stated in previous sections, the multi-dimensional experiments were not strictly necessary to accomplish this goal, but provided a valuable hands-on experience with interpretation and collection of multi-dimensional NMR.

References

- [1] Mark Robert Willcott. Mestre nova. *Journal of the American Chemical Society*, 131(36):13180–13180, 2009.
- [2] Sdbsweb : <https://sdbs.db.aist.go.jp>. *National Institute of Advanced Industrial Science and Technology*, 2019.
- [3] D Banfi and L Patiny. www.nmrdb.org: Resurrecting and processing nmr spectra on-line. *Chimia*, 62(4):280–281, 2008.
- [4] Christoph Steinbeck, Stefan Krause, and Stefan Kuhn. Nmrshiftdb constructing a free chemical information system with open-source components. *Journal of chemical information and computer sciences*, 43(6):1733–1739, 2003.
- [5] European Union. Regulation no. 1169/2011. *Official Journal of the Commission of the European Communities*. Available online: <http://eur-lex.europa.eu/legal-content/EN/TXT/?uri=uriserv:OJ.L.2011.304.01.0018.01.ENG>.
- [6] F Camin, A Pavone, L Bontempo, R Wehrens, M Paolini, A Faberi, RM Marianella, D Capitani, S Vista, and L Mannina. The use of irms, ^1H nmr and chemical analysis to characterise italian and imported tunisian olive oils. *Food Chem*, 196:98–105, 2016.
- [7] E Karkoula, A Skantzari, E Melliou, and P Magiatis. Quantitative measurement of major secoiridoid derivatives in olive oil using qnmr. proof of the artificial formation of aldehydic oleuropein and ligstroside aglycon isomers. *J. Agric. Food Chem*, 62:600–607, 2014.
- [8] G Dugo, A Rotondo, D Mallamace, N Cicero, A Salvo, E Rotondo, and C Corsaro. Enhanced detection of aldehydes in extra-virgin olive oil by means of band selective nmr spectroscopy. *Phys. A Stat. Mech. Appl*, 420:258–264, 2015.
- [9] P Dais and E Hatzakis. Quality assessment and authentication of virgin olive oil by nmr spectroscopy: A critical review. *Analytica Chimica Acta*, 765:1–27, 2013.
- [10] RP D’Amelia, L Huang, WF Nirode, E Rotman, J Shumila, and NM Wachter. Application of ^1H -nmr for the quantitative analysis of short chain fatty acid methyl ester mixtures: An undergraduate instrumental analysis experiment. *World Journal of Chemical Education*, 3(2):46–50, 2015.
- [11] JS Santos, GB Escher, JM da Silva Pereira, MT Marinho, LD Prado-Silva, AS Sant’Ana, LM Dutra, A Barison, and D Granato. ^1H nmr combined with chemometrics tools for rapid characterization of edible oils and their biological properties. *Industrial Crops and Products*, 116:191–200, 2018.
- [12] B Zhang, S Halouska, R Gaupp, S Lei, E Snell, RJ Fenton, RG Barletta, GA Somerville, and R Powers. Revisiting protocols for the nmr analysis of bacterial metabolomes. *J. Integr. OMICS*, 2:120–137, 2013.
- [13] HJ Reich. “8.1 relaxation in nmr spectroscopy.” 8.1 relaxation in nmr spectroscopy, university of wisconsin.